A new estimation of Numerical Diffusivity from Improved Tracer Variance Budget in Eddy-resolving Ocean Simulation

Jean-Michel Campin, Simone Silvestri and Raffaele Ferrari EAPS, MIT, Cambridge MA, USA (jmc@mit.edu),

1 Abstract

Quantifying how much mixing there is in ocean model solutions is essential for model evaluation and comparison because it is directly related to tracer distribution and water mass transformation, yet also affects the energetics through dissipation and potential energy production. A new tracer variance diagnostic (Banerjee et al., 2024) is used that distinguishes between transport and destruction in each direction thus allowing estimation, from the destruction term, of the numerical diffusivity in all directions. The method applies to any finite-volume discretization of the advection-diffusion equation and to most vertical coordinates since it accounts for the evolution of grid-cell thickness.
An idealized, southern-ocean-like eddy-resolving channel, similar to Hill et al. (2012), is used to evaluate the new method in comparison with others. Various advection schemes are considered, including those previously reported but also new high-order, weighted essentially non-oscillatory (WENO) advection schemes. By exploiting this method's specific capability, some averaged diagnostics including vertical profiles of variance destruction and effective diffusivity are presented. Methods to derive a diapycnal effective diffusivity are discussed and results are compared with other estimations.

2 Objective and Motivation

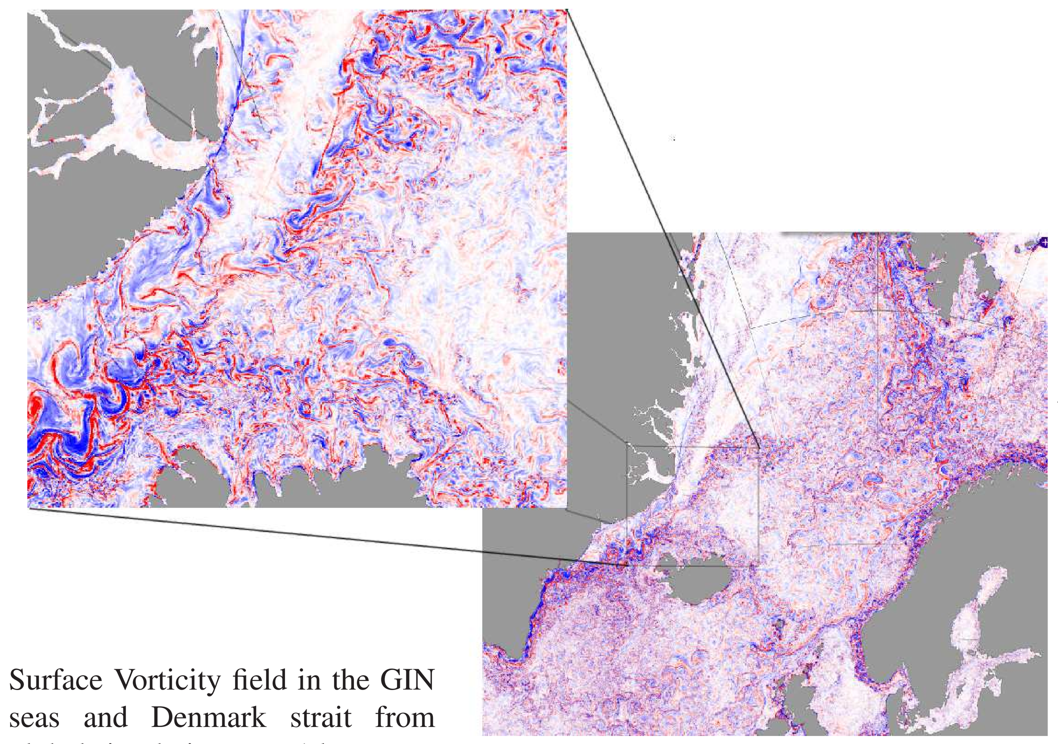

Surface Vorticity field in the GIN seas and Denmark strait from global simulation at $\simeq$ 1.km res.
(results from D. Menemenlis *etal*, 2014, using MITgcm on NASA-AMES computer; Figure from Ryan Abernathey)

Objective:

1. Provide a closed tracer variance budget that distinguishes between redistribution (transport) and production/destruction.
2. Fluid advection only contributes to variance transport. Diffusion contributes to both. $\Longrightarrow$ Estimate numerical diffusion (anywhere + in 3 directions) from the variance production.

Applications:

- analyze high resolution simulation (complex & very turbulent flow)
- compare with observations (tracer release)
- water-mass transformation
- evaluate numerical scheme (e.g., dependence on grid Reynolds number, Ilicak et al. (2011))

3 Method

In each grid cell, the tracer variance (σ^2):

$$\text{Rate of change}(\sigma^2) \;=\; \text{Transp}(\sigma^2) \;+\; \text{Prod}(\sigma^2)$$

The goal is to relate both terms to the model tracer equation, i.e., tracer advective flux assuming finite volume discretization.

Notations:

For any variable "q" and for any of the 3 dimensions x, y, z or time t, we define $\delta()$, $\overline{()}$ and $\widetilde{()}^2$ as:

$$\text{for} \quad i = x, y, z, t \quad : \qquad \delta^i q = q(i + \Delta i/2) - q(i - \Delta i/2) \ ;$$
$$\overline{q}^i = [q(i + \Delta i/2) + q(i - \Delta i/2)]/2 \ ; \ \widetilde{q}^{2i} = q(i + \Delta i/2) \times q(i - \Delta i/2)$$

The 3 components of the velocity vector are written (v_x, v_y, v_z) ; and for any grid-cell mesh $(\Delta x, \Delta y, \Delta z)$ the corresponding transport through each face of the grid-cell is $V_x = v_x \Delta y \Delta z$; $V_y = v_y \Delta x \Delta z$; $V_z = v_z \Delta x \Delta y$.

Using finite volume discretization, grid-cell volume "h" ($= \Delta x \Delta y \Delta z$) evolution relates to the continuity equation:

$$\delta^t h = -\Delta t \sum_{i=x,y,z} \delta^i V_i \qquad (1)$$

And tracer concentration "c" evolves according to:

$$\delta^t (hc) = -\Delta t \sum_{i=x,y,z} \delta^i F_i(V_i, c) \qquad (2)$$

where $F_i(V_i, c)$ is the advective flux of tracer concentration c in the direction i.

Variance budget:

The changes in tracer variance (here after take c^2 as σ^2) is:

$$\delta^t (hc^2) = -\widetilde{c}^{2t} \delta^t h + 2\overline{c}^t \delta^t (hc) \qquad (3)$$

Direct Method Banerjee et al. (2024), no residual :

$$\delta^t (hc^2) \;=\; -\, \Delta t \sum_{i=x,y,z} \delta^i \mathrm{T}_i \;+\; \Delta t \sum_{i=x,y,z} \overline{\mathrm{P}_i}^i \qquad (4)$$

$$\text{transport flux :} \quad \mathrm{T}_i \;=\; 2\overline{c}^{it} F_i - V_i \overline{(\widetilde{c}^{2t})}^i \qquad (5)$$
$$\text{production term :} \quad \mathrm{P}_i \;=\; 2F_i \, \delta^i \overline{c}^t - V_i \, \delta^i (\widetilde{c}^{2t}) \qquad (6)$$

Effective diffusivity:

Following Morales Maqueda and Holloway (2006), the effective diffusivity $[\kappa^\sigma]$ in each direction ($i = x, y, z$) is evaluated from the variance production term (eq.6) as:

$$\kappa_i^\sigma = \frac{-\mathrm{P}_i}{2(\delta^i c^t)^2} \frac{1}{\Delta d_i} \qquad (7)$$

with geometric factor $\Delta d_x = (\Delta y \Delta z)/\Delta x$ and similarly for Δd_y and Δd_z.

Direction splitting

Fractional time-stepping is often used (e.g. in MITgcm) to solve multi-dimensional advection equation. The advance in time from $t0$ to $t0 + \Delta t$ is splitted in three fractional steps: $t0 \rightarrow t1 \rightarrow t2 \rightarrow t3 = t0 + \Delta t$ with intermediate volume h^{t1}, h^{t2} and tracer concentration c^{t1}, c^{t2}:

$$\begin{array}{ll} \delta_x^t(hc) = (hc)^{t1} - (hc)^{t0} = -\Delta t \, \delta^x F_x(V_x, c^{t0}) & \delta_x^t h = h^{t1} - h^{t0} = -\Delta t \, \delta^x V_x \\ \delta_y^t(hc) = (hc)^{t2} - (hc)^{t1} = -\Delta t \, \delta^y F_y(V_y, c^{t1}) \ \text{with :} & \delta_y^t h = h^{t2} - h^{t1} = -\Delta t \, \delta^y V_y \\ \delta_z^t(hc) = (hc)^{t3} - (hc)^{t2} = -\Delta t \, \delta^z F_z(V_z, c^{t2}) & \delta_z^t h = h^{t3} - h^{t2} = -\Delta t \, \delta^z V_z \end{array}$$

To apply the previous method of tracer variance diagnostics to fractional time-stepping is straightforward. For instance T_x and P_x are evaluated (5 & 6) with the corresponding intermediate step tracer concentration: $\overline{c}^t = (c^{t0} + c^{t1})/2$ and $\widetilde{c}^{2t} = c^{t0} \times c^{t1}$; and similarly $\mathrm{T}_y, \mathrm{P}_y$ using c^{t1}, c^{t2} and $\mathrm{T}_z, \mathrm{P}_z$ using c^{t2}, c^{t3}.
And similarly, the numerical diffusivity is:

$$\kappa_x^\sigma = \frac{-\mathrm{P}_x}{2(\delta^x c^{t0})^2} \frac{1}{\Delta d_x} \ ; \ \kappa_y^\sigma = \frac{-\mathrm{P}_y}{2(\delta^y c^{t1})^2} \frac{1}{\Delta d_y} \ ; \ \kappa_z^\sigma = \frac{-\mathrm{P}_z}{2(\delta^z c^{t2})^2} \frac{1}{\Delta d_z} \qquad (8)$$

4 Eddying Channel application

For comparison, use the same set-up as Hill et al. (2012): Zonally re-entrant, flat bottom channel, 3.km deep, on Cartesian grid (β-plane) at 5.km resolution, forced by zonal wind, surface heat flux and temperature relaxation near Northern boundary. Use z^* coordinate (Adcroft and Campin, 2004), keep KPP mixing scheme but without non-local term, and use higher vertical resolution (90 Lev., $\max(\Delta z) = 42$) than reference 2012 set-up. Also run the same set-up (but without KPP) with Oceananigans (Ramadhan et al., 2020) using some high-order WENO schemes (Silvestri et al., 2024).

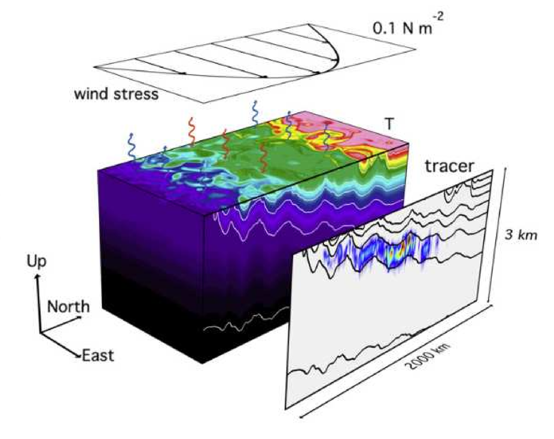

Perform variance budget analysis over the last 5 years of a 110.yr spin-up with the 3^{rd} order, direct space-time advection scheme with Sweby limiter (Hill et al., 2012)[A6]: budget closes perfectly after including forcing contribution ; variance destruction and effective diffusivity (over 5.yr and over L_x) are shown below for each direction.

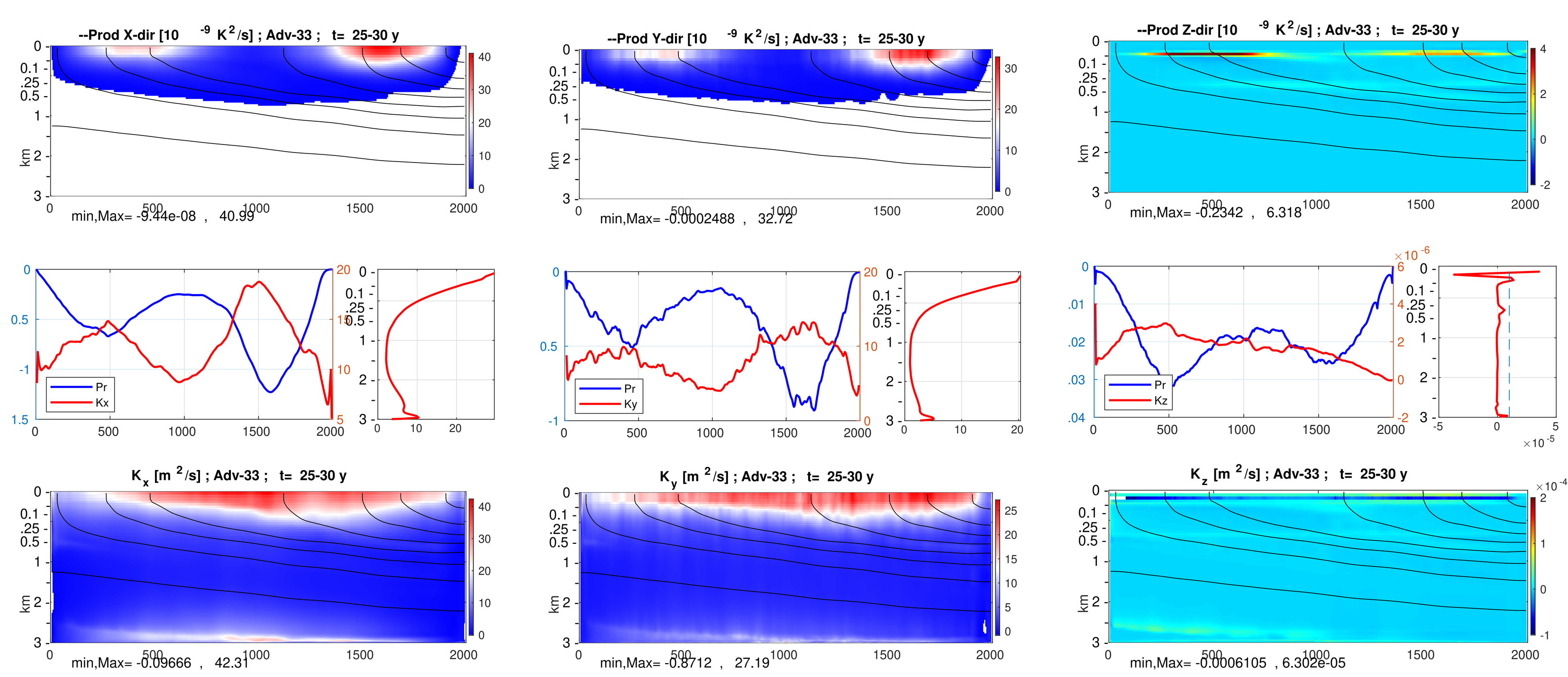

Findings: diffusivity are mostly positive in x and y directions but some negative destruction along z (specially in the surface mixed layer); smooth enough without extra averaging; and consistent with Hill et al. (2012) with caution (horizontal diffusivity is diapycnal).

5 Comparison

Comparison of diagnosed numerical diffusivity in the eddying channel using MITgcm or Oceananigans with various numerical schemes.

Oceananigans / MITgcm with and without KPP

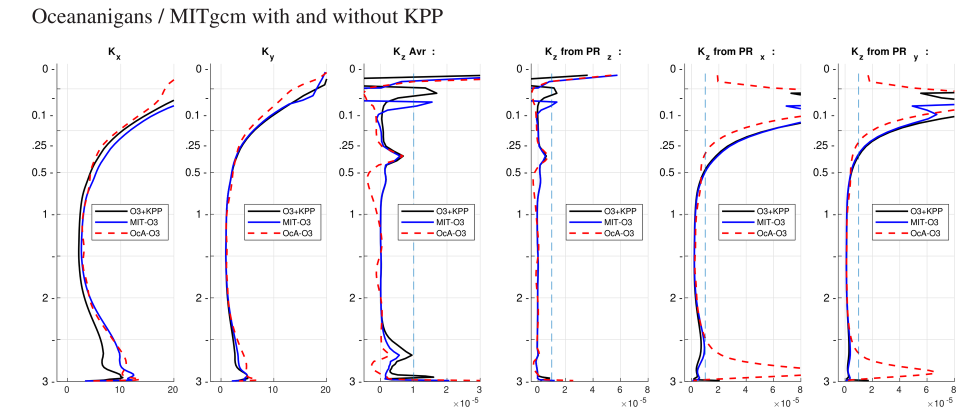

Using same diffusive 3^{rd}O upwind scheme: good agreement between the 2 models. Shear-instability near the bottom could explain larger diffusivity near the bottom (reduced with KPP).

Low diffusivity schemes (Hill et al., 2012)

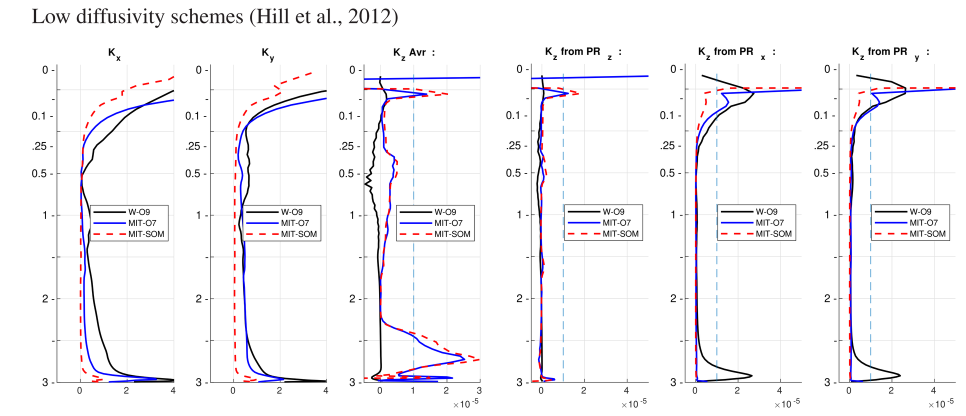

Numerical diffusivity strongly depends on advection scheme. Findings here confirm Hill et al. (2012) ranking with very low diffusion from the Second-Order Moment (SOM) scheme.

Reynolds number effect

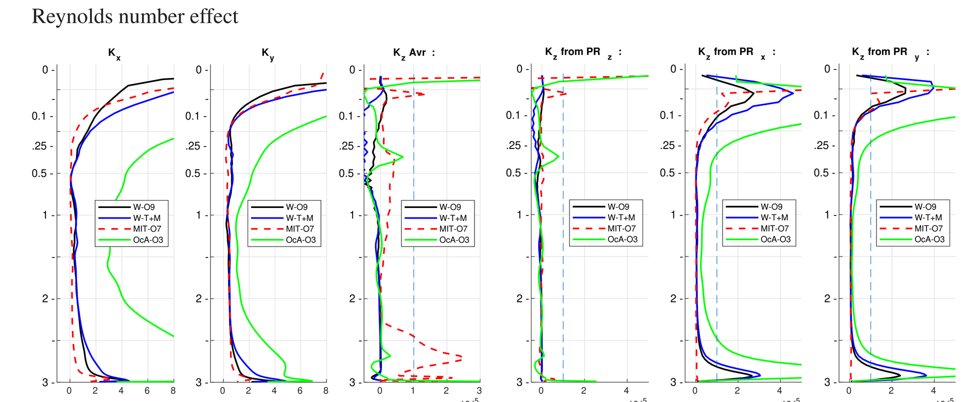

Using high order WENO for both Momentum and Tracer (Silvestri et al., 2024), here W-M+T curve, enhances fine structures in the flow field. The expected (Ilicak et al., 2011) increase of tracer numerical diffusivity here (vs prescribed horizontal hi-harmnic viscosity, W-O9) remains relatively small.

Apart from the problem with very coarse vertical resolution near the bottom, the diagnosed numerical diffusivity is not sensitive to vertical resolution as seen here with the 3^{rd}O scheme.

Vertical resolution (with 3^{rd}O scheme)

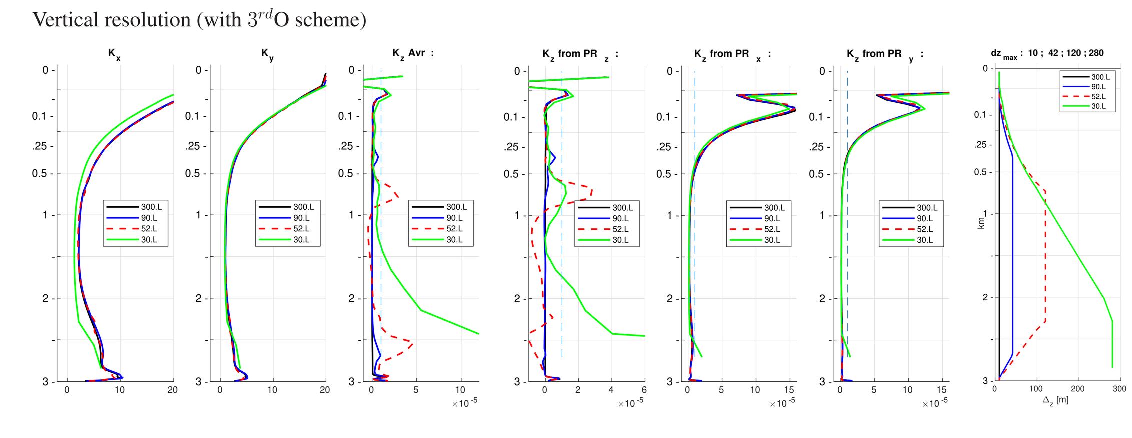

6 Conclusion

A new tracer variance diagnostic (Banerjee et al., 2024) distinguishes between transport and destruction in each direction thus allowing to quantify, from the destruction term, the numerical diffusivity in all directions. The method has been implemented in two ocean models and applied to an idealized eddying-channel simulation.

About the method:

- The diagnosed numerical diffusivity match previous estimations (Hill et al., 2012) obtained with different methods but with same model, in the same set-up and same numerical schemes. It confirms the large spreading from numerical schemes.
- Maps of numerical diffusivity in each direction are available.
- Despite different time-stepping, a good agreement is found between the two models when using the same (simple) 3^{rd} Order Upwind avection scheme.

And beyond:

- useful for understanding the model solution, e.g., the enhanced diffusivity near the bottom likely related to shear-instability.
- modest effect (larger diffusivity expected) from improving flow-field fine structures when switching from constant bi-harmonic viscosity to high-order WENO scheme for momentum.
- ready to be used in realistic global-ocean simulation.

References

Adcroft, A., Campin, J.-M., 2004. Re-scaled height coordinates for accurate representation of free-surface flows in ocean circulation models. *Ocean-Modelling*, **7**, 269-284, 2004.
Banerjee, T., Danilov, S., Klingbeil, K., Campin, J.-M., Discrete variance decay analysis of spurious mixing. *Ocean-Modelling*, **submitted**, 2024.
Hill, C., D. Ferreira, J.-M. Campin, J. Marshall, R. Abernathey, N. Barrier, Controlling spurious diapycnal mixing in eddy-resolving height-coordinate ocean models – Insights from virtual deliberate tracer release experiments *Ocean-Modelling*, **45-46**, 14-26, 2012.
Ilicak, M., A. Adcroft, S. M. Griffies, and R. Hallberg, 2012: Spurious dianeutral mixing and the role of momentum closure. *Ocean Modelling*, **37-58**, 14-26, 2012.
Holmes, R. M., Zika, J. D., Griffies, S. M., Hogg, A. M., Kiss, A. E., and England, M. H., 2021: The geography of numerical mixing in a suite of global ocean models. *JAMES*, **13**, doi: 10.1029/2020MS002333
Klingbeil, K., Mohammadi-Aragh, M., Grawe, U., Burchard, H., 2014. Quantification of spurious dissipation and mixing - discrete variance decay in a finite-volume framework. *Ocean-Modelling*, **81**, 49-64, 2014.
Silvestri, Simone, G. Wagner, J.-M. Campin, N. Constantinou, C. Hill, A. Souza and R. Ferrari, 2024, A new WENO-based momentum advection scheme for simulations of ocean mesoscale turbulence. *JAMES*, **16**, doi: 10.1029/2023MS004130